Computers & Structures Vol. 18, No. 3, pp. 537–549, 1984
Printed in Great Britain.

0045–7949/84 $3.00 + .00

PROBABILITY OF FAILURE MODELS IN FINITE ELEMENT ANALYSIS OF BRITTLE MATERIALS

CONSTANTINOS GEORGIADIS
SINTEF, The Foundation of Scientific and Industrial Research at the Norwegian Institute of Technology, Trondheim, Norway

(*Received* 3 *November* 1982; *received for publication* 17 *January* 1983)

Abstract—A model of failure for brittle materials is presented, based on the weakest link hypothesis and Weibull distribution function. Methods of computing the probability of failure of a structural component, and numerical implementation in a finite element program, are shown. Computer subroutines are included.

1. INTRODUCTION

In recent years, due to new developments in aerospace engineering and energy efficient engines, the demand for materials operating in high temperatures has increased. As a result the study of *ceramic* materials has been rapidly taking new dimensions.

The fundamental characteristics of *ceramic or brittle materials* are that they show no plastic deformations before failure and they have little toughness to arrest cracks. Thus, there is a need for a different design procedure than that of the familiar engineering materials.

More details about the characteristics, properties, developments, and design methods of brittle materials can be found in Refs. [1–4].

When designing with brittle materials an important factor is the computation of the reliability or probability of survival of a structural component under certain loading conditions. The computation of stresses using finite element analysis is the basis for this. Therefore a further extension of finite element programs to include a probability of survial computation would be useful.

In this report a model of failure, based on the weakest link hypothesis and Weibull statistics, is presented. The model is investigated for different stress situations, and is implemented in a finite element analysis. Appropriate computer subroutines, and flow charts for implementation in existing general purpose programs are shown.

Linear elastic material properties are assumed through all this report.

2. WEIBULL MODEL OF FAILURE

A Weibull model of failure[5, 6], is based on the assumption that flaws are distributed at random with certain density per unit volume. The failure is based on the "weakest link hypothesis", which states that a component will fail when the stress intensity at any flaw reaches a critical value for crack propagation. Thus the structural component is represented as a series model or a chain, with components being small parts of the structure, in which the failure depends on the weakest component.

For the expression of the probability of failure a Weibull distribution[7] is used, and the *probability of failure* of a small volume $\mathrm{d}V$ under a normal tensile stress σ is computed as:

$$P_f(\mathrm{d}V) = 1 - \exp\left[-\left(\frac{\sigma}{\sigma_0}\right)^m \mathrm{d}V\right] \qquad (2.1)$$

where σ_0 and m are material constants. The way they can be estimated from experimental data is shown in Refs. [1, 2, 4].

Sometimes, the material can withstand a threshold stress σ_u without failure. Then eqn (2.1) takes the form

$$P_f(\mathrm{d}V) = 1 - \exp\left[-\left(\frac{\sigma - \sigma_u}{\sigma_0}\right)^m \mathrm{d}V\right]. \qquad (2.1a)$$

In this work, here, the commonly accepted assumption that $\sigma_u = 0$ is made, and eqn (2.1) will be used.

The *probability of survival* of a volume $\mathrm{d}V$ is expressed as:

$$P_s(\mathrm{d}V) = \exp\left[-\left(\frac{\sigma}{\sigma_0}\right)^m \mathrm{d}V\right] \qquad (2.2)$$

and the *risk of rupture*

$$S(\mathrm{d}V) = \left(\frac{\sigma}{\sigma_0}\right)^m \mathrm{d}V. \qquad (2.3)$$

According to the failure model, the probability of survial of an assembly of volumes is:

$$P_s(V) = \prod_V P_S(\mathrm{d}V) \qquad (2.4)$$

where $\prod_V$ designates a product extended over the volume V.

The risk of rupture of a volume V is

$$S(V) = \int_V \left(\int_{\Delta V} \frac{1}{\Delta V}\left(\frac{\sigma_n}{\sigma_0}\right)^m \mathrm{d}V\right)\Delta V \qquad (2.5)$$

where the first integral is over a small volume ΔV around a point, and σ_n is the normal tensile stress under which a small region $\mathrm{d}V/\Delta V$ at this point is. The second integral is over the volume of the structural component.

3. RELATIONS FOR VARIOUS STRESS SITUATIONS

Before we proceed further into the numerical evaluation of eqn (2.5), in conjuction with finite element analysis, it is reasonable to look at certain stress situations, and obtain the forms of the integral over ΔV in eqn (2.5).

3.1 *Triaxial stress*

In the case of a volume ΔV around a point O subjected to a triaxial stress, characterized by the three principal stresses, σ_1, σ_2, σ_3 (Fig. 1a), the normal stress on a plane (n) is:

$$\sigma_n = \sigma_1 \sin^2 \Theta \cos^2 \Phi + \sigma_2 \sin^2 \Theta \sin^2 \Phi + \sigma_3 \cos^2 \Phi. \tag{3.1}$$

Assuming a volume $\mathrm{d}V = (r^3/3) \sin \Theta \,\mathrm{d}\Theta \,\mathrm{d}\Phi$ (Fig. 1b) under this stress the risk of rupture for the volume ΔV according to eqn (2.5) is:

$$S(\Delta V) = \frac{\Delta V}{4\pi} \int_0^{2\pi} \mathrm{d}\Phi \int_0^{\pi} \left(\frac{\sigma_1}{\sigma_0} \sin^2 \Theta \cos^2 \Phi + \frac{\sigma_2}{\sigma_0} \sin^2 \Theta \sin^2 \Phi + \frac{\sigma_3}{\sigma_0} \cos^2 \Phi \right)^m \sin \Theta \,\mathrm{d}\Theta. \tag{3.2}$$

In the case of equiaxial tension, $\sigma_1 = \sigma_2 = \sigma_3 = \sigma$ eqn (3.2) yields:

$$S(\Delta V) = \left(\frac{\sigma}{\sigma_0} \right)^m \Delta V. \tag{3.3}$$

3.2 *Biaxial stress*

In the case of biaxial stress, (Fig. 2) $\sigma_3 = 0$, eqn (3.2) becomes:

$$S(\Delta V) = \frac{\Delta V}{4\pi} \int_0^{2\pi} \left(\frac{\sigma_1}{\sigma_0} \cos^2 \Phi + \frac{\sigma_2}{\sigma_0} \sin^2 \Phi \right)^m \mathrm{d}\Phi \times \int_0^{\pi} \sin \Theta^{2m+1} \,\mathrm{d}\Theta \tag{3.4}$$

and (see Appendix A)

$$S(\Delta V) = \frac{\Delta V m \Gamma(m)}{2\surd(\pi)(2m+1)\Gamma(m+\frac{1}{2})} \int_0^{2\pi} \left(\frac{\sigma_1}{\sigma_0} \cos^2 \Phi + \frac{\sigma_2}{\sigma_0} \sin^2 \Phi \right)^m \mathrm{d}\Phi. \tag{3.5}$$

Plane stress. For the plane stress situation, the stress does not vary along the thickness, so integrating eqn (3.5) over the thickness the risk of rupture for a small area ΔA around a point O is

$$S(\Delta A) = \Delta A h \frac{m \Gamma(m)}{2\surd(\pi)(2m+1)\Gamma(m+\frac{1}{2})} \int_0^{2\pi} \left(\frac{\sigma_1}{\sigma_0} \cos^2 \Phi + \frac{\sigma_2}{\sigma_0} \sin^2 \Phi \right)^m \mathrm{d}\Phi. \tag{3.6}$$

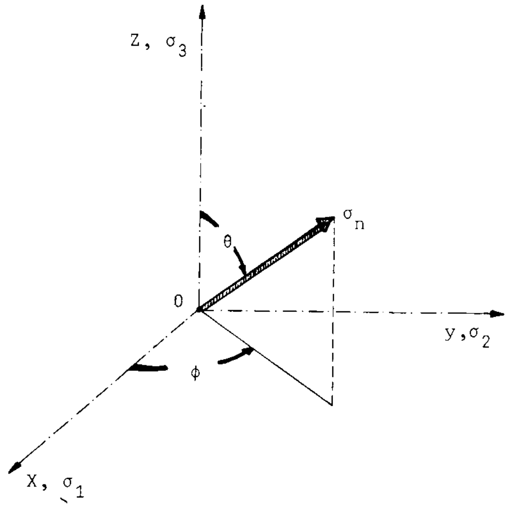

Fig. 1(a).

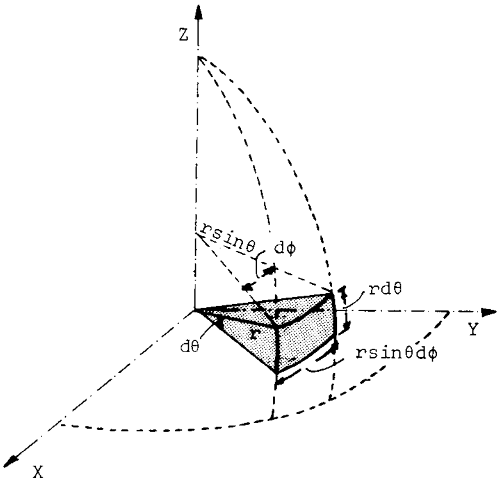

Fig. 1(b).

Plate bending. In the case of plate bending, the stresses vary linearly along the thickness, so from eqn (3.5) is obtained for the risk of rupture of an area ΔA

$$\begin{aligned} S(\Delta A) &= \frac{\Delta A m \Gamma(m)}{2\surd(\pi)(2m+1)\Gamma(m+\frac{1}{2})} \int_0^{h/2} \mathrm{d}z \times \int_0^{2\pi} \left(\frac{2z}{h} \frac{\sigma_1}{\sigma_0} \cos^2 \Phi + \frac{2z}{h} \frac{\sigma_2}{\sigma_0} \sin^2 \Phi \right)^m \mathrm{d}\Phi \\ &= \frac{\Delta A h m \Gamma(m)}{4\surd(\pi)(m+1)(2m+1)\Gamma(m+\frac{1}{2})} \times \int_0^{2\pi} \left(\frac{\sigma_1}{\sigma_0} \cos^2 \Phi + \frac{\sigma_2}{\sigma_0} \sin^2 \Phi \right)^m \mathrm{d}\Phi \end{aligned} \tag{3.7}$$

where σ_1, σ_2 are principal stresses on the tension surface of the plate.

Torsion of a bar. In the case of pure torsion of a bar (Fig. 3), a volume ΔV at distance r from the axis x–x is under biaxial state of stress, $\sigma_1 = \tau$, $\sigma_2 = -\tau$, where τ is the shearing stress at that point. From eqn (3.5) the

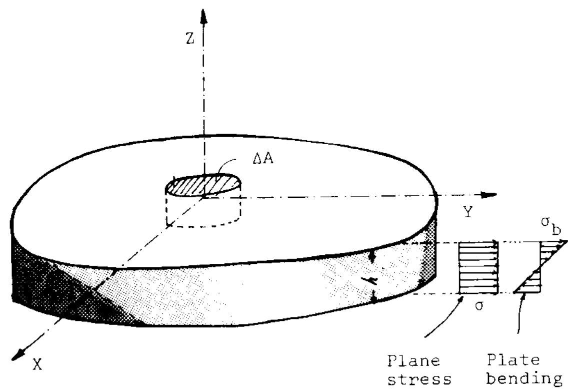

Fig. 2.

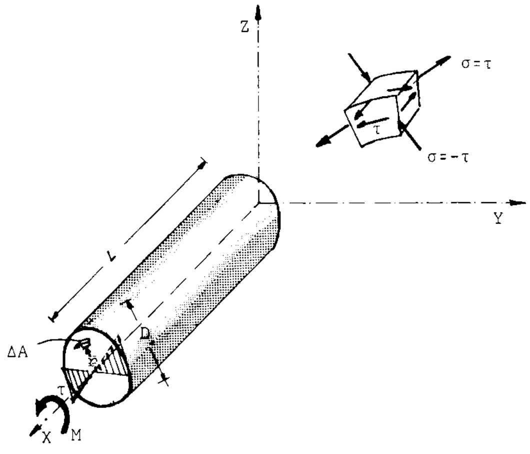

Fig. 3.

risk of rupture for a volume $\Delta V = \Delta A\,\Delta x$ is computed as:

$$S(\Delta V) = \Delta A\,\Delta x\frac{m\Gamma(m)}{2\sqrt{(\pi)}(2m+1)\Gamma(m+\frac{1}{2})}\left(\frac{\tau}{\sigma_0}\right)^m \times \int_0^{2\pi}(\cos^2\Phi - \sin^2\Phi)^m\,\mathrm{d}\Phi \qquad (3.8)$$

and (see Appendix C)

$$S(\Delta V) = \Delta A\,\Delta x\frac{2\Gamma(m)\Gamma(m/2+\frac{1}{2})}{(2m+1)\Gamma(m+\frac{1}{2})\Gamma(m/2)}\left(\frac{\tau}{\sigma_0}\right)^m. \qquad (3.9)$$

For a circular cross section the variation of shearing stresses is linear $\tau = (2r/D)\tau_m$, where τ_m is the maximum shearing stress, and integrating eqn (3.9) over the cross section, the risk of rupture becomes.

$$\begin{aligned} S(\Delta x) &= \Delta x\frac{2\Gamma(m)\Gamma(m/2+\frac{1}{2})}{(2m+1)\Gamma(m+\frac{1}{2})\Gamma(m/2)} \times 2\pi\int_0^{D/2}\left(\frac{2r}{D}\frac{\tau_m}{\sigma_0}\right)^m \mathrm{d}r \\ &= \Delta xD\frac{2\pi\Gamma(m)\Gamma(m/2+\frac{1}{2})}{(m+1)(2m+1)\Gamma(m+\frac{1}{2})\Gamma(\frac{1}{2})}\left(\frac{\tau_m}{\sigma_0}\right)^m. \end{aligned} \qquad (3.10)$$

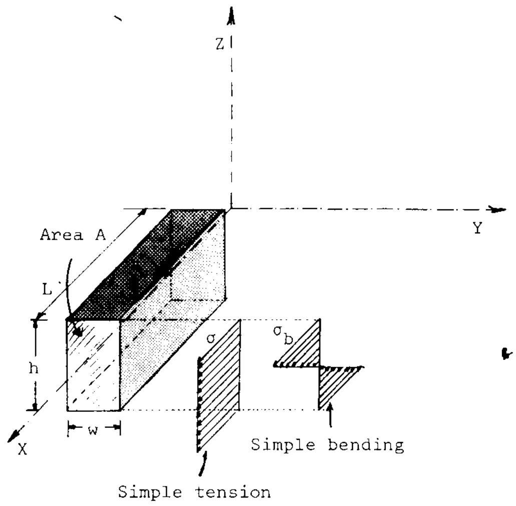

Fig. 4.

3.3 *Uniaxial stress*

In the case of uniaxial stress state (Fig. 4), $\sigma_2 = \sigma_3 = 0$, eqn (3.2) reduces to:

$$S(\Delta V) = \Delta V\left(\frac{\sigma_1}{\sigma_0}\right)^m\int_0^{2\pi}\cos\Phi^{2m}\,\mathrm{d}\Phi \times \int_0^{\pi}\sin\Theta^{2m+1}\,\mathrm{d}\Theta \qquad (3.11)$$

and (see Appendix A)

$$S(\Delta V) = \Delta V\frac{1}{(2m+1)}\left(\frac{\sigma_1}{\sigma_0}\right)^m. \qquad (3.12)$$

Uniaxial tension. Tensile stress is constant, equal to σ over the cross section, and eqn (3.12) yields:

$$S(\Delta x) = \Delta x\frac{A}{(2m+1)}\left(\frac{\sigma}{\sigma_0}\right)^m. \qquad (3.13)$$

Simple bending of rectangular cross section. Stress varies linearly over the cross section and eqn (3.12) becomes:

$$S(\Delta x) = \Delta x \frac{1}{(2m+1)} \int_0^{h/2} \left(\frac{2z}{h}\frac{\sigma_b}{\sigma_0}\right)^m w\,\mathrm{d}z$$

$$= \Delta x \frac{wh}{2(m+1)(2m+1)} \left(\frac{\sigma_b}{\sigma_0}\right)^m. \qquad (3.14)$$

3.4 *General remarks*

Sometimes an additional assumption is made for the flaws around a material point, instead of random uniform distribution. This assumption is based on the fact, that flaws on the surface of the material can sometimes dominate the probability of failure.

So it can be assumed that for thin plate-like specimens flaws are formed only perpedicular to the plane of the plate, and for bar-like specimens flaws are formed only perpedicular to the axis of the bar. This results in different values for the risk of rupture as follows:

Biaxial stress:

$$S^*(\Delta V) = \frac{\Delta V}{2\pi} \int_0^{2\pi} \left(\frac{\sigma_1}{\sigma_0}\cos^2\Phi + \frac{\sigma_2}{\sigma_0}\sin^2\Phi\right) \mathrm{d}\Phi. \qquad (3.15)$$

Uniaxial stress:

$$S^*(\Delta V) = \Delta V \left(\frac{\sigma}{\sigma_0}\right)^m. \qquad (3.16)$$

Comparing the above relations with eqn (3.5) and (3.12) the following ratios for the risk of rupture are obtained:

Biaxial stress:

$$\rho_1 = \frac{S(\Delta V)}{S^*(\Delta V)} = \frac{\ln P_s(\Delta V)}{\ln P_s^*(\Delta V)} = \frac{m\Gamma(m)\sqrt{(\pi)}}{(2m+1)\Gamma(m+\frac{1}{2})}. \qquad (3.17)$$

Uniaxial stress:

$$\rho_2 = \frac{S(\Delta V)}{S^*(\Delta V)} = \frac{\ln P_s(\Delta V)}{\ln P_s^*(\Delta V)} = \frac{1}{2m+1}. \qquad (3.18)$$

The coefficients ρ_1 and ρ_2 are plotted in (Fig. 5) for various values of the Weibull modulus *m*.

4. FINITE ELEMENT MODEL

In a Finite element model of the structure, with displacement formulation, the displacements inside an element $(i, j, k, \ldots)$ (Fig. 6), are expressed as [8]:

$$\mathbf{u}(\mathbf{r}) = \begin{Bmatrix} u^x(\mathbf{r}) \\ u^y(\mathbf{r}) \\ u^z(\mathbf{r}) \end{Bmatrix} = [\mathbf{N}_i^e, \mathbf{N}_j^e, \ldots] \begin{Bmatrix} \mathbf{d}_i \\ \mathbf{d}_j \\ \vdots \end{Bmatrix}^e = \mathbf{N}^e\mathbf{d}^e \quad (4.1)$$

where

$$\mathbf{N}_i^e = N_i^e\mathbf{I} \qquad (4.2a)$$

N_i^e: element shape functions; **I**: a (3×3) identity matrix taking care of the three coordinate directions, *x*, *y*, *z*.

$$\mathbf{d}_i = \begin{Bmatrix} d_i^x \\ d_i^y \\ d_i^z \end{Bmatrix} \text{:nodal displacements of node } i. \, (4.2\text{b})$$

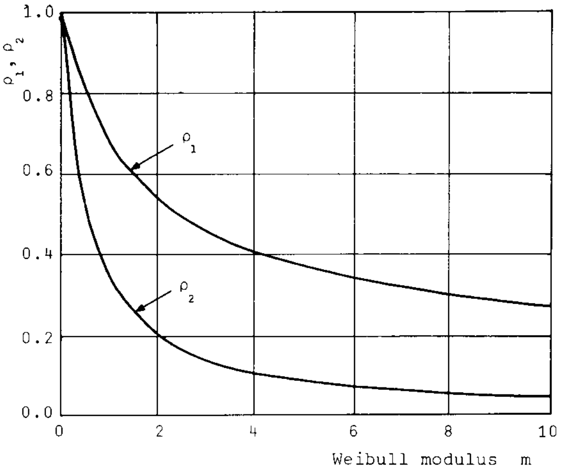

Fig. 5.

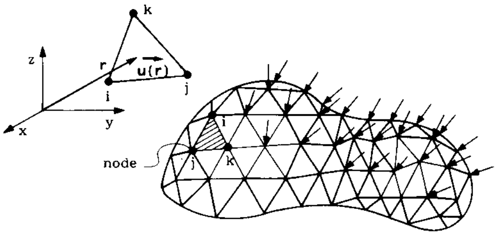

Fig. 6.

The superscript *e* designates that the corresponding matrices contain all the submatrices for a particular element *e*.

The strains of any point of the element can be determined from the nodal displacements as

$$\boldsymbol{\epsilon} = \mathbf{B}\mathbf{d}^e \qquad (4.3)$$

where

$$\mathbf{B} = \mathbf{L}\mathbf{N}^e \qquad (4.4a)$$

and **L** is a suitable linear operator[8].

The components of stress for a linear elastic element are obtained from the strains

$$\boldsymbol{\sigma} = \mathbf{D}(\boldsymbol{\epsilon} - \boldsymbol{\epsilon}_0) + \boldsymbol{\sigma}_0 \qquad (4.5)$$

where **D** is an elastic matrix containing the appropriate material properties, ϵ_0 and σ_0 are initial strains and stresses correspondingly.

After a finite element solution the nodal displacements are calculated and the stresses inside an element can be expressed using the nodal displacements as:

$$\boldsymbol{\sigma} = \mathbf{D}\mathbf{B}\mathbf{d}^e - \mathbf{D}\boldsymbol{\epsilon}_0 + \boldsymbol{\sigma}_0. \qquad (4.6)$$

From the above stress tensor at a point the normal stress at any direction can be obtained as

$$\sigma_n = \mathbf{T}\boldsymbol{\sigma} \tag{4.7}$$

where T is a transformation matrix.

For the computation of the probability of failure in a finite element model, eqn (2.5) takes the form:

$$S(V) = \sum_{k=1}^{N_e} \int_{V_k} \left(\int_{\Delta V} \frac{1}{\Delta V} \left(\frac{\sigma_n}{\sigma_0} \right)^m \mathrm{d}V \right) \Delta V \tag{4.8}$$

where N_e is the number of elements.

For each element the stresses are computed at the Gauss quadrature points, so the integral over the volume of each element will be evaluated with a Gauss numerical integration scheme as

$$\int_{V_k} \left(\int_{\Delta V} \frac{1}{\Delta V} \left(\frac{\sigma_n}{\sigma_0} \right)^m \mathrm{d}V \right) \Delta V = \underset{\substack{\uparrow \\ \text{Element} \\ \text{volume}}}{V_k} \sum_{i=1}^{M} \underset{\substack{\nwarrow \\ \text{Integration} \\ \text{weights}}}{W_i} \underbrace{\left(\int_{\Delta V} \frac{1}{\Delta V} \left(\frac{\sigma_n}{\sigma_0} \right)^m \mathrm{d}V \right)_i}_{\substack{\text{Evaluated at Gauss} \\ \text{quadrature points}}} . \tag{4.9}$$

The way the risk of rupture is computed for various element of a finite element library is summarized in the following Table 1.

Appendix B summarizes some numerical integration methods for the computation of the integral over the volume ΔV in eqn (4.9).

Appendix C presents a computer subroutine computing the probability of failure for the elements presented in Table 1. The same appendix shows how this subroutine can be included in a general purpose finite element program.

5. CONCLUSIONS

In the present work a model of failure for brittle materials, based on the weakest link hypothesis, has been presented. The Weibull distribution has been used to obtain the probability of failure of a structural component.

The numerical implementation and the inclusion in a general purpose finite element program of the above model has been shown, with appropriate computer subroutines and flow charts.

Examples and results of applications of the method to various practical situations and correlation with experimental data can be found in Refs. [9–12].

It is evident that models like the above, for computing the probability of failure of structural components, should be included in the various finite element programs.

Table 1.

ELEMENT	*STRESS SITUATION*	*RISK OF RUPTURE COMPUTATION*
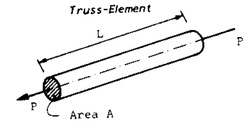	$\sigma = \frac{P}{A}$	$S = \frac{AL}{(2m+1)} \left(\frac{P}{A\sigma_0}\right)^m$
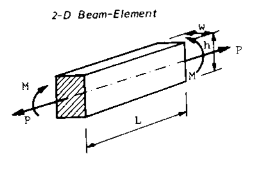	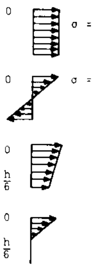$M = 0$ $\sigma = \frac{P}{A}$ $P = 0$ $\sigma = \frac{M}{\frac{wh^2}{6}}$ $P > 0$ $\frac{M}{P} \leqslant \frac{h}{6}$ $P < 0$ $\frac{M}{P} \geqslant \frac{h}{6}$	$S = \frac{whL}{(2m+1)} \left(\frac{P}{wh\sigma_0}\right)^m$ $S = \frac{whL}{2(m+1)(2m+1)} \left(\frac{6M}{wh^2\sigma_0}\right)^m$ $S = \frac{w^2h^3L\sigma_0}{12M(m+1)(2m+1)} \left[\left(\frac{P}{wh\sigma_0} + \frac{6M}{wh^2\sigma_0}\right)^{m+1} - \left(\frac{P}{wh\sigma_0} - \frac{6M}{wh^2\sigma_0}\right)^{m+1} \right]$ $S = \frac{w^2h^3L\,\sigma_0}{12M(m+1)(2m+1)} \left(\frac{P}{wh\sigma_0} + \frac{6M}{wh^2\sigma_0}\right)^{m+1}$
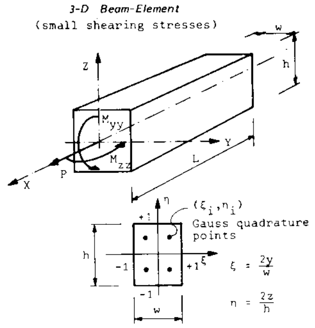	$\sigma = \frac{P}{wh} + \frac{6M_{yy}}{wh^2}\eta + \frac{6M_{zz}}{hw^2}\xi$	$S = \frac{whL}{4(2m+1)} \sum_{i=1}^{M} \sum_{j=1}^{M} \underset{\substack{\uparrow \\ \text{Gauss} \\ \text{integration} \\ \text{weights}}}{W_i W_j} \underbrace{\left(\frac{P}{wh\sigma_0} + \frac{6M_{yy}}{wh^2\sigma_0}\eta + \frac{6M_{zz}}{hw^2\sigma_0}\xi\right)}_{\substack{\text{Stress evaluated at} \\ \text{Gauss quadrature points} \\ \text{If it is negative for a} \\ \text{point is set equal to zero}}}^m$

Table 1 (*Contd*).

ELEMENT	*STRESS SITUATION*	*RISK OF RUPTURE COMPUTATION*
Plane stress element 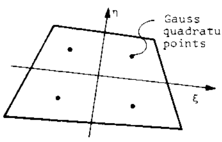 ξ, η :Normal coordinates A :area, h :thickness	$\sigma = \sigma_1 \cos^2\phi + \sigma_2 \sin^2\phi$ $\sigma_3 = 0$	$S = \frac{A\ h\ m\ \Gamma(m)}{8\sqrt{\pi}(2m+1)\Gamma(m+\frac{1}{2})} \sum_{i=1}^{M} \sum_{j=1}^{M} W_i W_j\ T(\xi_i,\eta_j)$ $T(\xi_i,\eta_j) = \int_0^{2\pi} (\frac{\sigma_1}{\sigma_0} \cos^2\phi + \frac{\sigma_2}{\sigma_0} \sin^2\phi)^m\ d\ \phi$ where : σ_1 ,σ_2 are evaluated at Gauss quadrature point ξ_i,η_j. Numerical evaluation of the above integral for $T(\xi_i,\eta_j)$ as in Appendix B.
Plane strain element 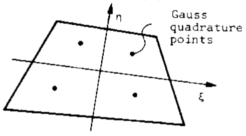	$\sigma = \sigma_1 \cos^2\phi + \sigma_2 \sin^2\phi$ σ_3 = constant	$S = \frac{A\ h}{16\pi} \sum_{i=1}^{M} \sum_{j=1}^{M} W_i W_j\ T(\xi_i,\eta_j)$ $T(\xi_i,\eta_j) = \int_0^{2\pi} d\phi \int_0^{\pi} (\frac{\sigma_1}{\sigma_0} \sin^2\theta \cos^2\phi + \frac{\sigma_2}{\sigma_0} \sin^2\theta \sin^2\phi + \frac{\sigma_3}{\sigma_0} \cos^2\phi)^m \sin\theta\ d\ \theta$ where : σ_1 ,σ_2 are evaluated at Gauss quadrature point ξ_i,η_j. Numerical evaluation of the above integral for $T(\xi_i,\eta_j)$ as in Appendix B.
Plate bending element 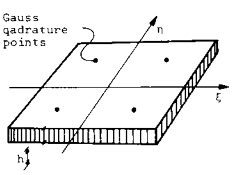	$\sigma_1 = M_1/\frac{h^3}{6}$ $\sigma_2 = M_2/\frac{h^3}{6}$ M_1 M_2 principal bending moments	$S = \frac{A\ h\ m\ \Gamma(m)}{16\sqrt{\pi}(m+1)(2m+1)\Gamma(m+\frac{1}{2})} \sum_{i=1}^{M} \sum_{j=1}^{M} W_i W_j\ T(\xi_i,\eta_j)$ $T(\xi_i,\eta_j) = \int_0^{2\pi} (\frac{6M_1}{h^3\sigma_0} \cos^2\phi + \frac{6M_2}{h^3\sigma_0} \sin^2\phi)^m d\phi$ where : M_1,M_2 are evaluated at Gauss quadrature point ξ_i,η_j. Numerical evaluation of the above integral for $T(\xi_i,\eta_j)$ as in Appendix B.
Axisymmetric element 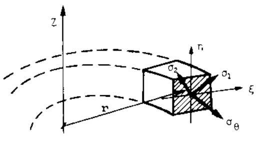 A : cross-section area ξ,η : normal coordinates of the cross section r : distance from axis of revolution	$\sigma = \sigma_1 \cos^2\phi + \sigma_2 \sin^2\phi$ σ_θ = constant with circumferential direction	$S = \frac{A}{8} \sum_{i=1}^{M} \sum_{j=1}^{M} W_i W_j r(\xi_i,\eta_j) T(\xi_i,\eta_j)$ $T(\xi_i,\eta_j) = \int_0^{2\pi} d\phi \int_0^{\pi} (\frac{\sigma_1}{\sigma_0} \sin^2\theta \cos^2\phi + \frac{\sigma_2}{\sigma_0} \sin^2\theta \sin^2\phi + \frac{\sigma_\theta}{\sigma_0} \cos^2\phi)^m \sin\theta d\theta$ where σ_1, σ_2, σ_θ are evaluated at Gauss quadrature point (ξ_i,η_j) of the cross section Numerical evaluation of the above integral for $T(\xi_i,\eta_j)$ as in Appendix B. $r(\xi_i,\eta_j)$: distance from axis of revolution of Gauss quadrature point (ξ_i,η_j).
3-D element 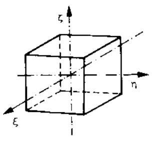 V : volume of element ξ,η,ζ : normal coordinates	σ_1, σ_2, σ_3 triaxial stress	$S = \frac{V}{32\pi} \sum_{i=1}^{M} \sum_{j=1}^{M} \sum_{k=1}^{M} W_i W_j W_k T(\xi_i,\eta_j,\zeta_k)$ $T(\xi_i,\eta_j,\zeta_k) = \int_0^{2\pi} d\phi \int_0^{\pi} (\frac{\sigma_1}{\sigma_0} \sin^2\theta \cos^2\phi + \frac{\sigma_2}{\sigma_0} \sin^2\theta \sin^2\phi + \frac{\sigma_3}{\sigma_0} \cos^2\phi)^{m} \sin\theta d\theta$ where σ_1, σ_2, σ_3 are evaluated at Gauss quadrature point ξ_i,η_j,ζ_k of the cross section. Numerical evaluation of the above integral for $T(\xi_i,\eta_j,\zeta_k)$ as in Appendix B.

Work for more sophisticated models of failure and extension to other kind of materials and structures, in addition to ceramic materials, is needed. Fatigue, deterioration, imperfections, and other phenomena could be looked upon as candidates for modelling in similar ways.

REFERENCES

1. J. Mueller, A. Kobayashi and D. Scott (Eds.), Design with brittle materials. College of Engineering, University of Washington, Seattle, Wash. (1979).
2. W. H. Dukes, *Handbook of Brittle Material Design Technology*. North Atlantic Treaty Organization, Advisory Group for Aerospace Research and Development AGARDograph (1970).
3. B. Lawn and T. Wilshaw, *Fracture of Brittle Solids*. Cambridge University Press, Cambridge (1975).
4. R. Taggart, Ceramic materials and structural applications. Brittle Material Design Group, College of Engineering, University of Washington, Seattle, Wash. (1981).
5. W. Weibull, A statistical theory of the strength of materials. Ingeniörs Vetenskaps Akademiens Handlingar No. 151, Stockholm (1939).
6. W. Weibull, *A Survey of Statistical Effects in the Field of*

Material Failure. Applied Mechanics Surveys. Spartan, New York (1966).
7. K. Bury, *Statistical Models in Applied Science.* Wiley, New York (1975).
8. O. C. Zienkiewicz, *The Finite Element Method*, 3rd Ed. McGraw-Hill, New York (1977).
9. F. Gac, *et al.*, Design analysis of an automotive exhaust gas sensor. *Ceramic Engng and Sci. Proc.* **1**(7–8) (1980).
10. TPS model study. *Special Status Rep.* 1. Brittle material design group, College of Engineering, University of Washington, Seattle, Wash. (1980).
11. TPS model study. *Special Status Rep.* 2. Brittle material desing group, College of Engineering, University of Washington, Seattle, Wash. (1980).
12. TPS model study. *Special Rep.* 3. Brittle material design group, College of Engineering, University of Washington, Seattle, Wash. (1981).
13. M. Abramowitz and I. Stegun, *Handbook of Mathematical Functions.* Dover, New York (1972).

APPENDIX A

Some useful mathematical expressions

Reference [13] has been used as a basic source.

$$2\int_0^{\pi/2} (\sin\Phi)^{2z-1}(\cos\Phi)^{2w-1}\,\mathrm{d}\Phi = \frac{\Gamma(z)\Gamma(w)}{\Gamma(z+w)} \quad \text{(A1)}$$

where z, $w > 0$, $\Gamma(z)$: gamma function.

The following relations, used in the previous text, are obtained from eqn (A1).

$$\int_0^{\pi/2} (\sin\Phi)^{2m+1}\,\mathrm{d}\Phi = \frac{1}{2}\frac{\Gamma(m+1)\Gamma(\frac{1}{2})}{\Gamma(m+3/2)} = \frac{\sqrt{(\pi)}m\Gamma(m)}{(2m+1)\Gamma(m+\frac{1}{2})} \quad \text{(A2)}$$

$(z = m + 1, w = \frac{1}{2})$

$$\int_0^{\pi/2} (\cos\Phi)^{2m}\,\mathrm{d}\Phi = \frac{1}{2}\frac{\Gamma(\frac{1}{2})\Gamma(m+\frac{1}{2})}{\Gamma(m+1)} = \frac{\sqrt{(\pi)}\Gamma(m+\frac{1}{2})}{2m\Gamma(m)} \quad \text{(A3)}$$

$(z = \frac{1}{2}, w = m + \frac{1}{2})$

$$\int_0^{\pi/4} (\cos^2\Phi - \sin^2\Phi)^m\,\mathrm{d}\Phi = \int_0^{\pi/4} (\cos 2\Phi)^m\,\mathrm{d}\Phi$$

$$= \frac{1}{2}\int_0^{\pi/2} (\cos\Theta)^m\,\mathrm{d}\Theta = \frac{1}{2}\frac{\Gamma\left(\frac{1}{2}\right)\Gamma\left(\frac{m+1}{2}\right)}{\Gamma\left(\frac{m}{2}+1\right)}$$

$$= \frac{\sqrt{(\pi)}\Gamma(m/2+\frac{1}{2})}{m\Gamma\left(\frac{m}{2}\right)} \quad \text{(A4)}$$

$\left(z = \frac{1}{2}, w = \frac{m+1}{2}\right).$

APPENDIX B

Numerical integration procedures for computing the risk of rupture of an elementary material volume

The numerical evaluation of the integrals appearing in eqn (3.5) and (3.2) is examined.

(I)

$$\int_0^{2\pi}\left(\frac{\sigma_1}{\sigma_0}\cos^2\Phi + \frac{\sigma_2}{\sigma_0}\sin^2\Phi\right)^m \mathrm{d}\Phi$$

$$= 4\int_0^{\pi/2}\left(\frac{\sigma_1}{\sigma_0}\cos^2\Phi + \frac{\sigma_2}{\sigma_0}\sin^2\Phi\right)^m \mathrm{d}\Phi = 4\int_0^{\pi/2} f(\Phi)\,\mathrm{d}\Phi. \quad \text{(B1)}$$

Using Gauss integration scheme we have (Fig. B1).

$$4\int_0^{\pi/2} f(\Phi)\,\mathrm{d}\Phi = \pi\sum_{i=1}^{n} W_i f(\Phi_i)$$

where n: number of Gauss quadrature points; W_i: integration weights; $\Phi_i = (\pi/4) + x_i(\pi/4)$; x_i: abscisas of the ith zero of the orthogonal polynomials. Values of W_i and x_i can be found in Ref. [13].

(II)

$$\int_0^{2\pi}\mathrm{d}\Phi\int_0^{\pi}\left(\frac{\widetilde{\sigma}_1}{\sigma_0}\sin^2\Theta\cos^2\Phi + \frac{\sigma_2}{\sigma_0}\sin^2\Theta\sin^2\Phi + \frac{\sigma_3}{\sigma_0}\cos^2\Phi\right)^m$$

$$\times \sin\Theta\,\mathrm{d}\Theta = 4\int_0^{\pi/2}\mathrm{d}\Phi\int_0^{\pi/2} f(\Phi,\Theta)\sin\Theta\,\mathrm{d}\Theta. \quad \text{(B2)}$$

For the numerical integration of eqn (B2) the formulae developed by Hammer *et al.*[8], for a triangular region of integration have been modified and presented in Table B1 for the integration on a surface of a sphere (Fig. B2).

It should be mentioned, that in the above integrations only the positive values (only tensilve stresses) of the integrated function contribute.

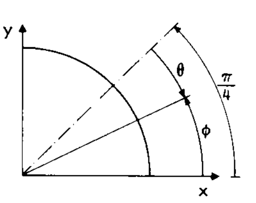

Fig. B1.

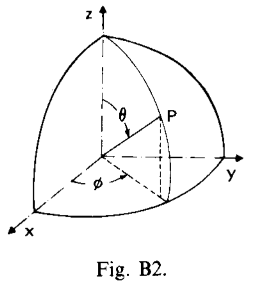

Fig. B2.

Table B1. Numerical integration formulae for spherical surface domain

$$\int_0^{\pi/2}\int_0^{\pi/2} f(\phi,\theta)\sin\theta d\phi d\theta = \frac{\pi}{2}\sum_{1}^{N} f(\phi_i,\theta_i)W_i$$

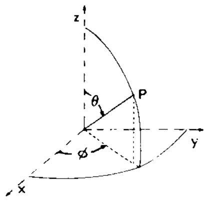

ORDER	FIGURE	POINTS N	POLAR COORDINATES IN DEGREES		WEIGHTS W_i
			ϕ_i	θ_i	
LINEAR	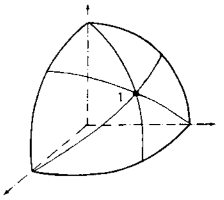	1	45.00000	60.00000	1.00000
QUADRATIC	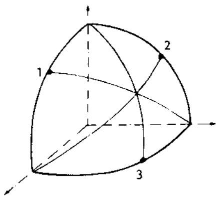	1	0.00000	45.00000	0.33333
		2	90.00000	45.00000	0.33333
		3	45.00000	90.00000	0.33333
CUBIC	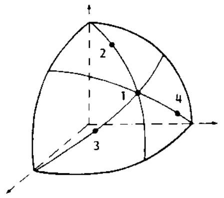	1	45.00000	60.00000	-0.56249
		2	45.00000	36.00000	0.52083
		3	27.19153	65.44120	0.52083
		4	62.80847	65.44120	0.52083
CUBIC	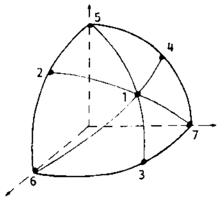	1	45.00000	60.00000	0.45001
		2	0.00000	45.00000	0.13333
		3	45.00000	90.00000	0.13333
		4	90.00000	45.00000	0.13333
		5	45.00000	0.00000	0.05000
		6	0.00000	90.00000	0.05000
		7	90.00000	90.00000	0.05000
QUINTIC	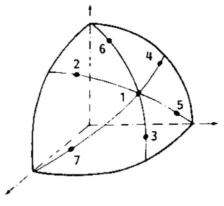	1	45.00000	60.00000	0.22501
		2	7.57846	45.25133	0.13239
		3	45.00000	84.62557	0.13239
		4	82.42154	45.25133	0.13239
		5	76.88862	77.21905	0.12594
		6	45.00000	18.23157	0.12594
		7	13.11138	77.21905	0.12594

APPENDIX C

Computer Program

The computation of the probability of failure in a general purpose finite element program can be done as is shown in the following flowchart (Fig. C1) and the computer subroutines.

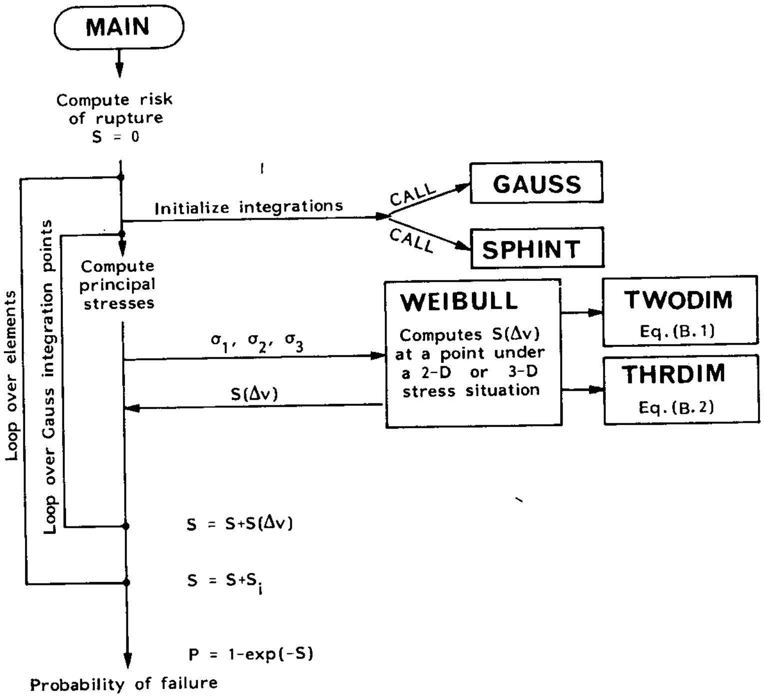

Fig. C1. Flowchart for computing the probability of failure.